Supporting Information

Confinement Chemistry of FeO_x Centers for Activating Molecular Oxygen under Ambient Condition

Bingqi Han, Xinbo Li, Zhibin Geng, Liping Li*, Guangshe Li*

State Key Laboratory of Inorganic Synthesis and Preparative Chemistry, College of Chemistry, Jilin University, Changchun 130012, P. R. China

e-mail: guangshe@jlu.edu.cn; lipingli@jlu.edu.cn

Content

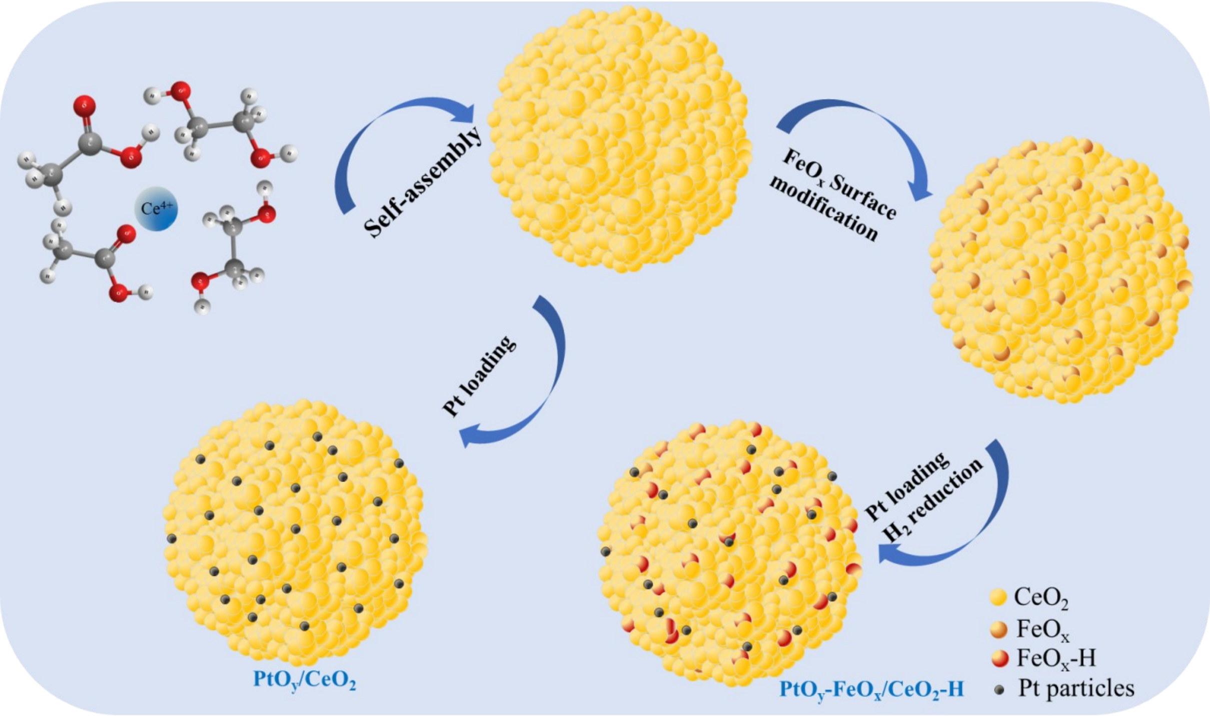

Figure S1. Schematic illustration of catalyst preparation

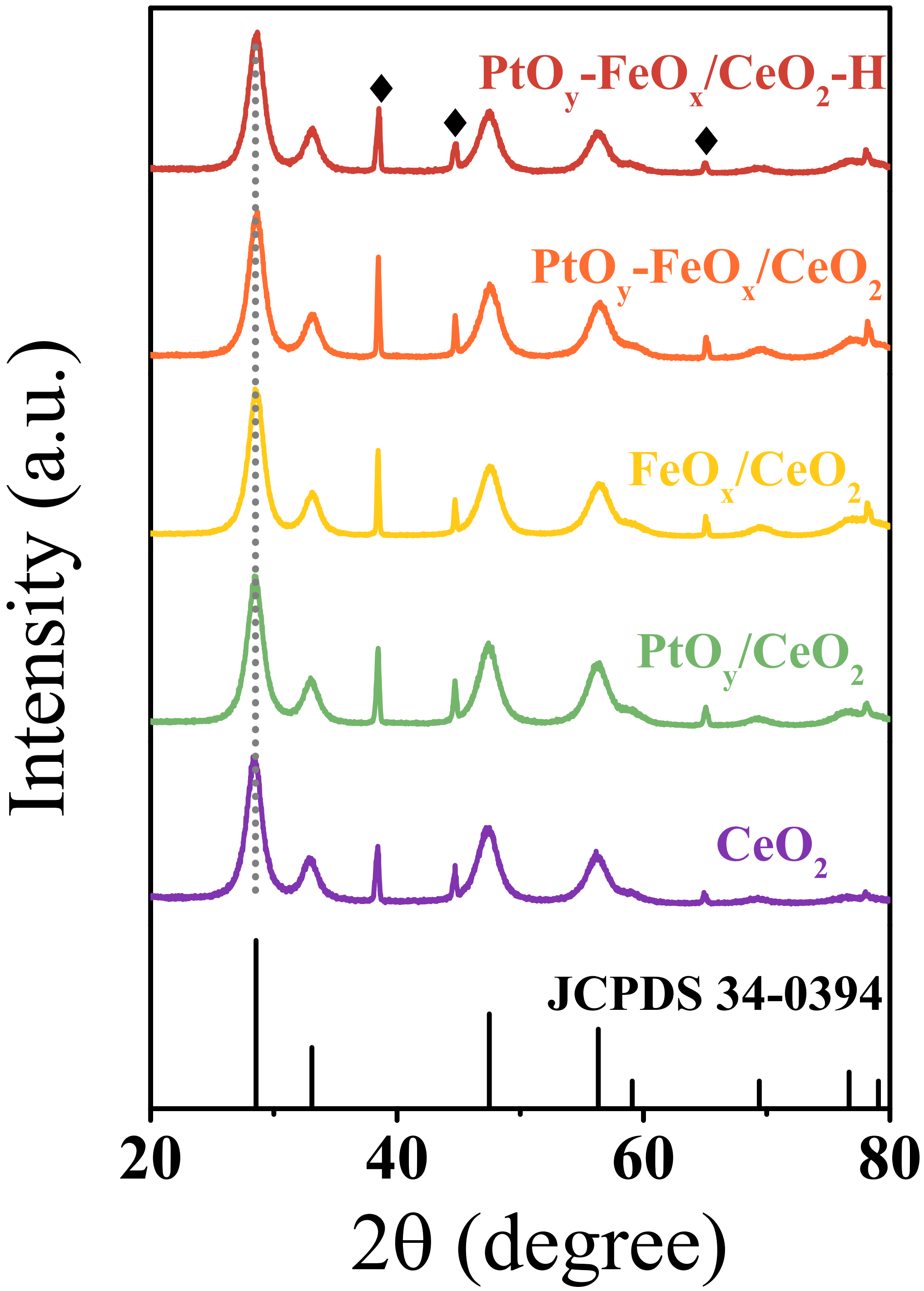

Figure S2. XRD patterns of the samples.

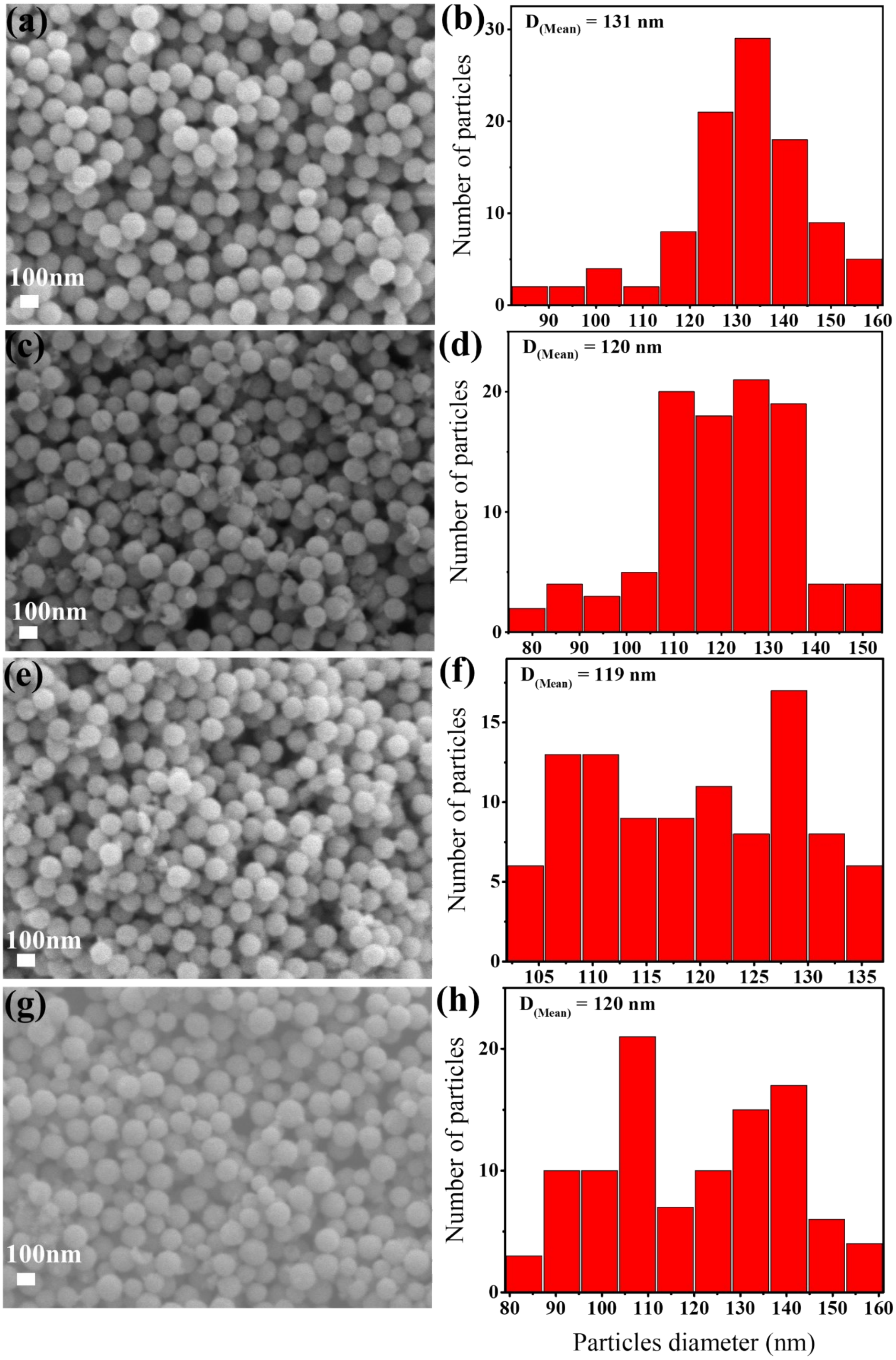

Figure S3. SEM images and statistical distribution of diameter of the samples: (a, b) CeO_2, (c, d) FeO_x/CeO_2, (e, f) PtO_y-FeO_x/CeO_2, and (g, h) PtO_y-FeO_x/CeO_2-H.

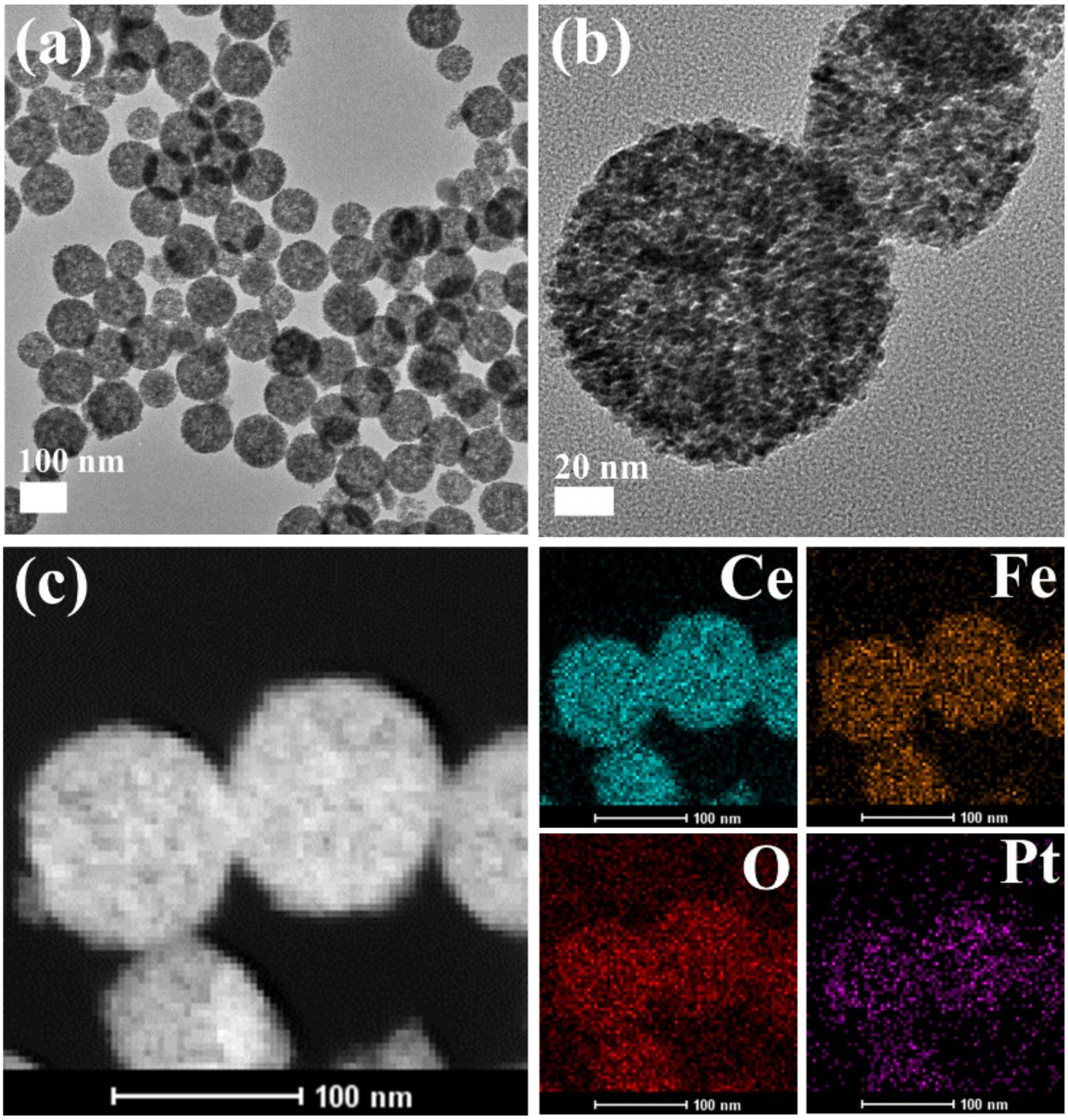

Figure S4. (a) TEM, (b) HR-TEM images, and (c) EDS mapping of PtO_y-FeO_x/CeO_2.

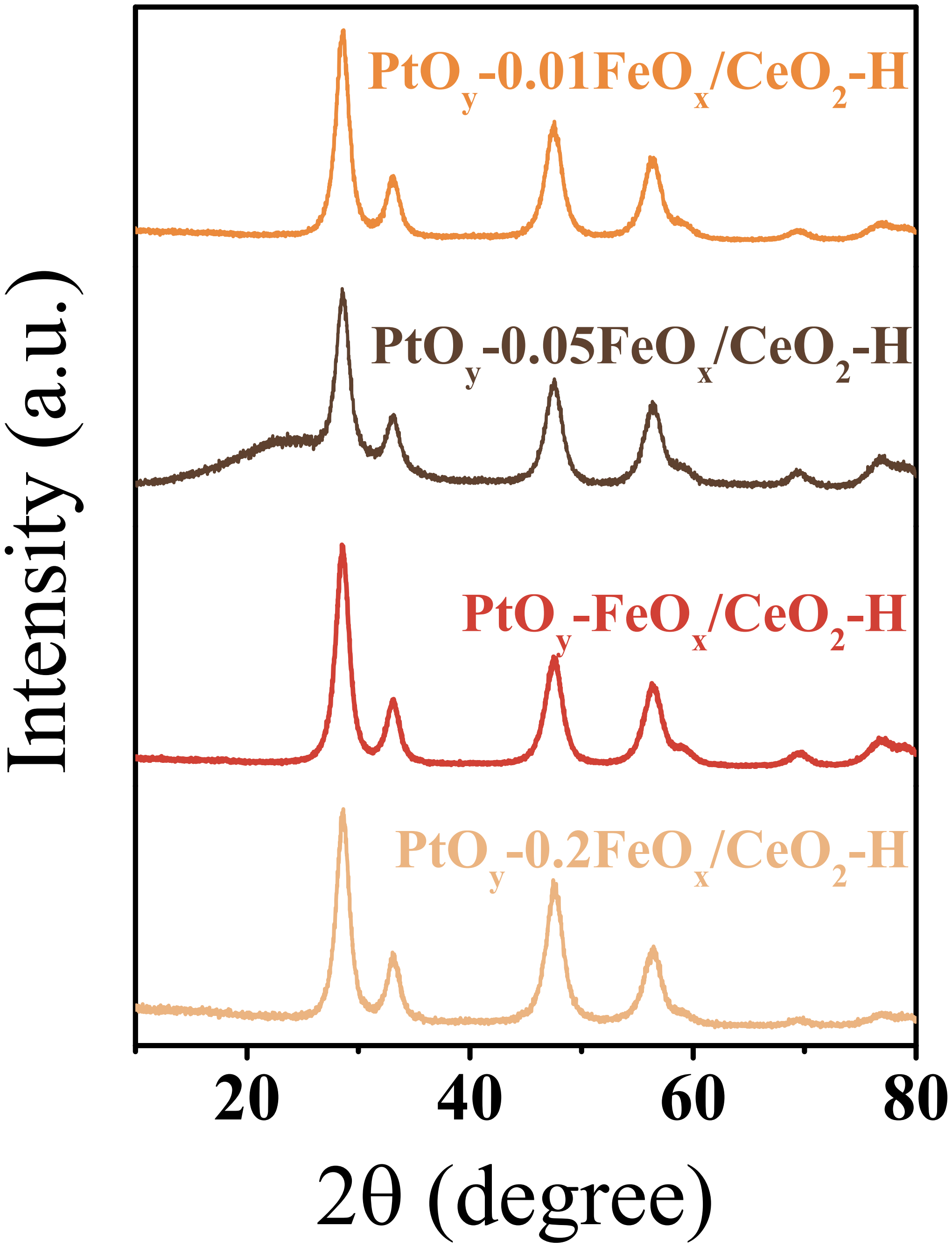

Figure S5. XRD patterns of PtO$_y$-FeO$_x$/CeO$_2$-H and PtO$_y$-mFeO$_x$/CeO$_2$-H (m=0.01, 0.05, and 0.2)

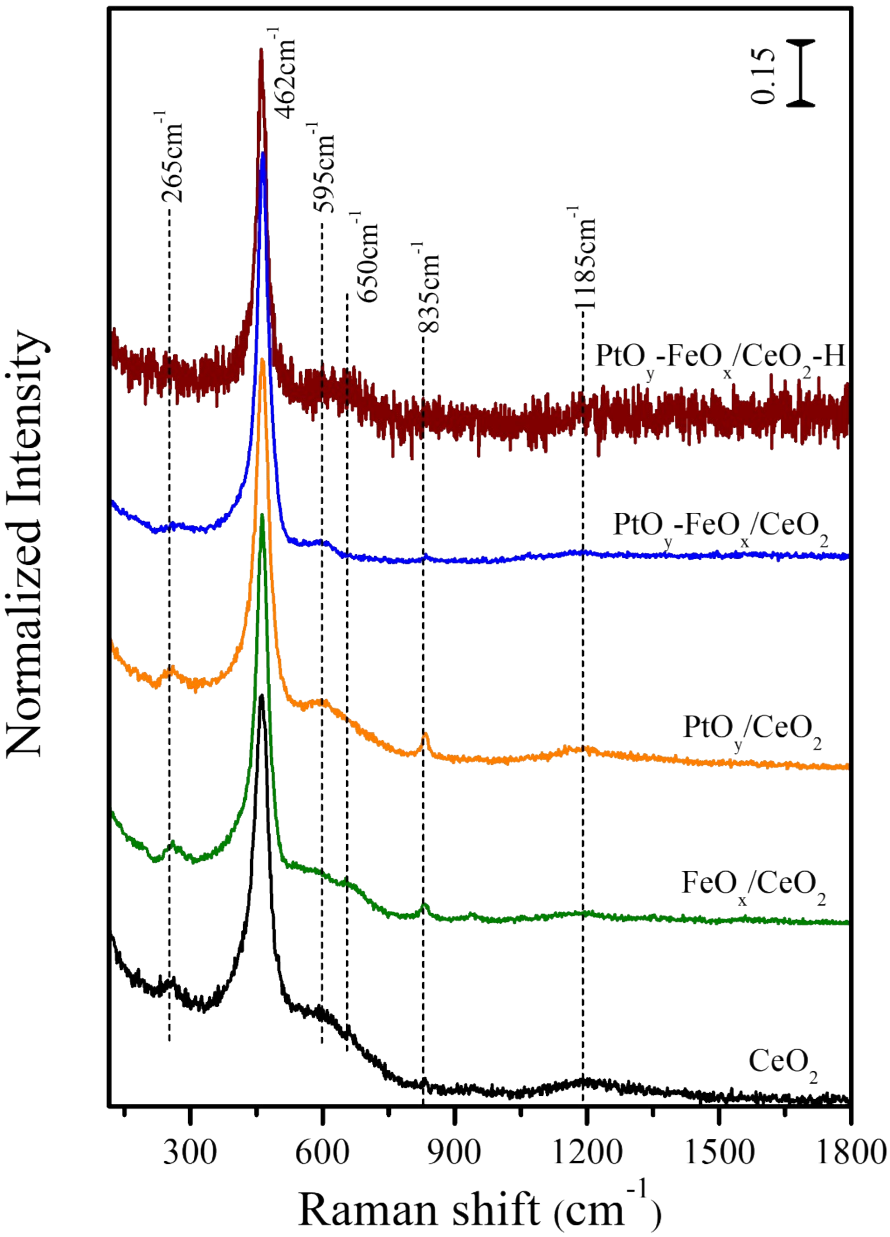

Figure S6. Raman spectra of the samples using 532 nm excitation.

Raman spectrum is a useful tool to detect ceria crystalline changes, such as lattice dilation effect with a proportional lower frequency shift from foreign ion doping, oxygen vacancy identification. Raman pattern is mainly composed of two peaks from F_{2g} mode (460 cm^{-1}) and a vibration caused by oxygen vacancy (580 cm^{-1}), as well as some weak second-order vibrations of CeO_2 (265，835 and 1185 cm^{-1})[1,2,3]

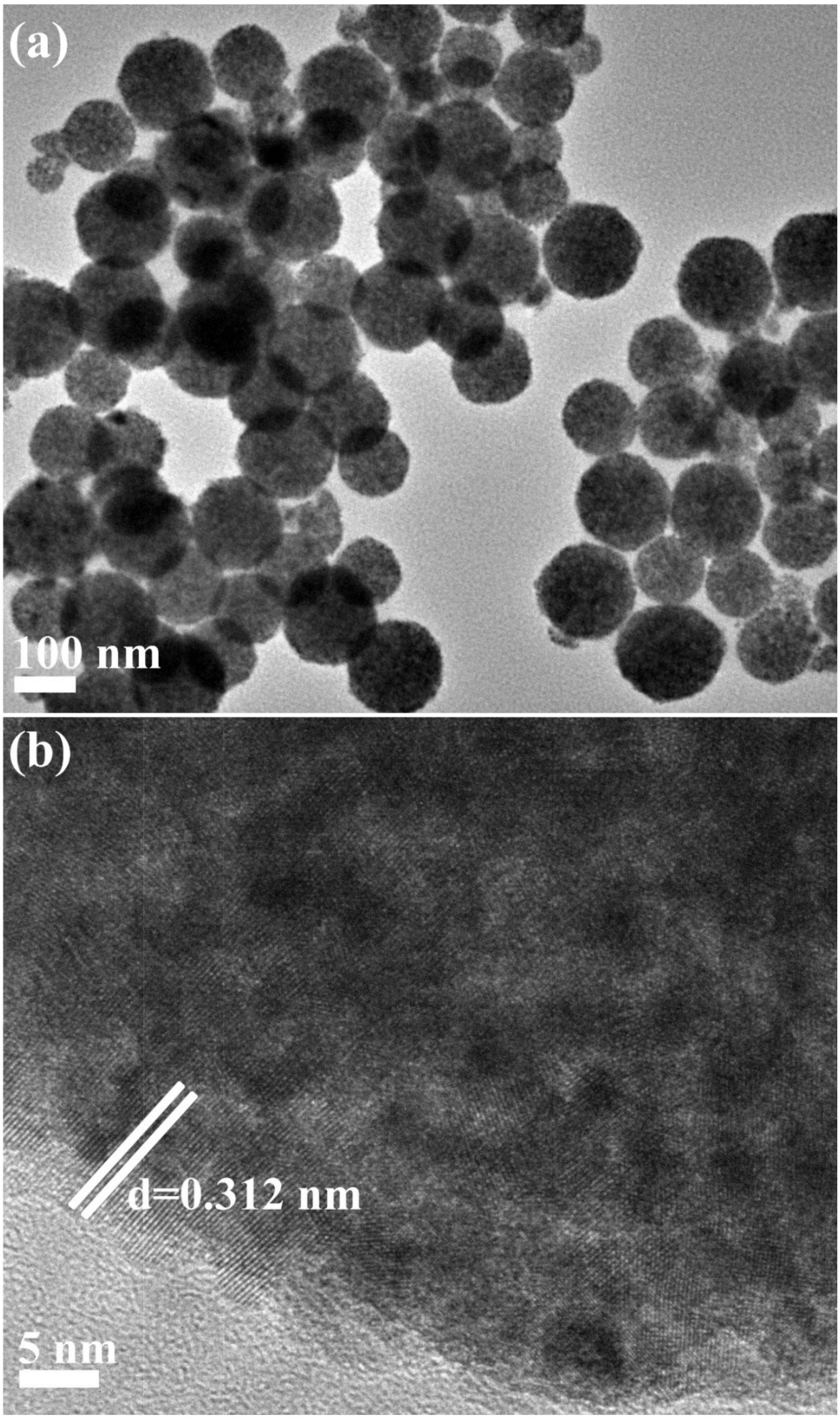

Figure S7. TEM image of PtO_y-FeO_x/CeO_2-H.

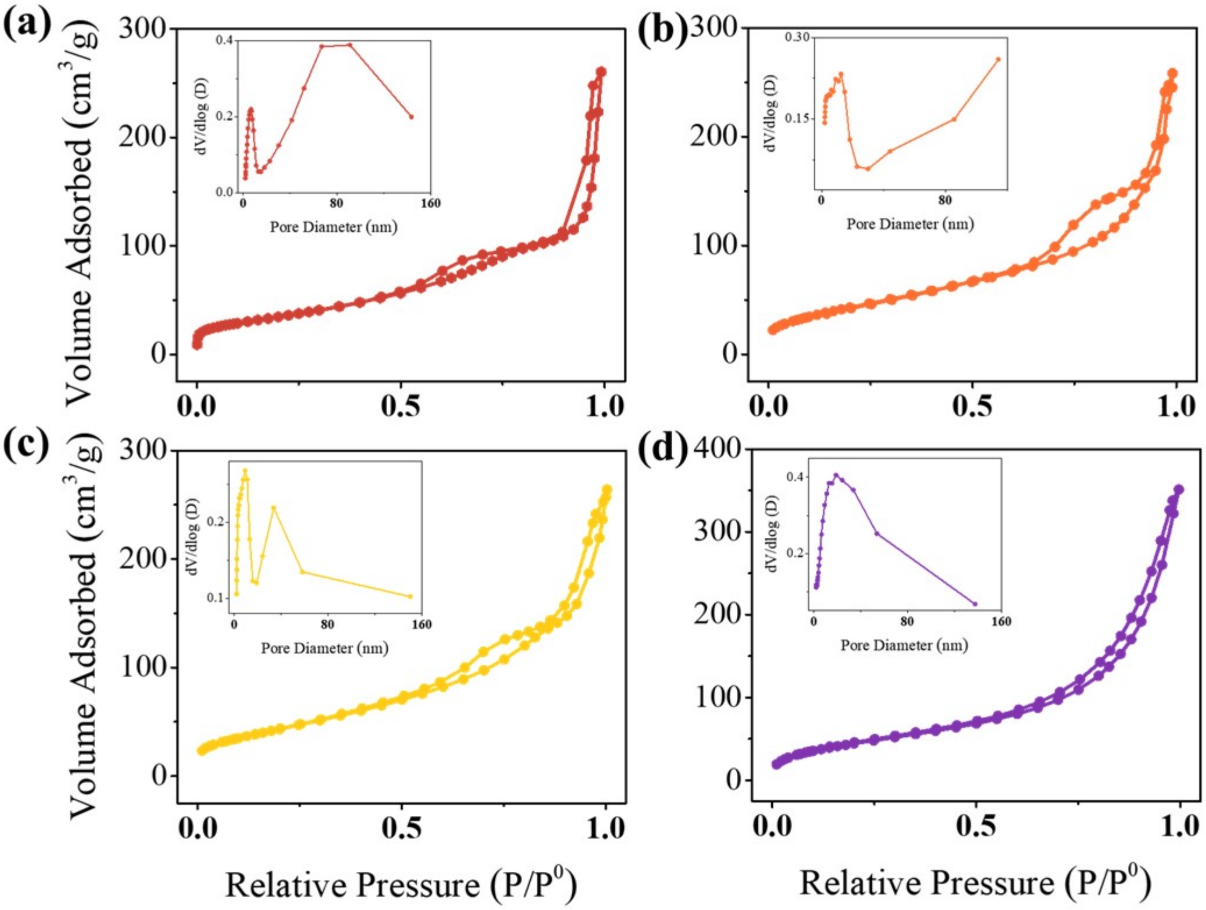

Figure S8. N_2 adsorption desorption isotherms of the samples: (a) PtO_y-FeO_x/CeO_2-H, (b) PtO_y-FeO_x/CeO_2, (c) FeO_x/CeO_2, and (d) CeO_2. Inserted figures are the BJH pore size distribution curves of samples.

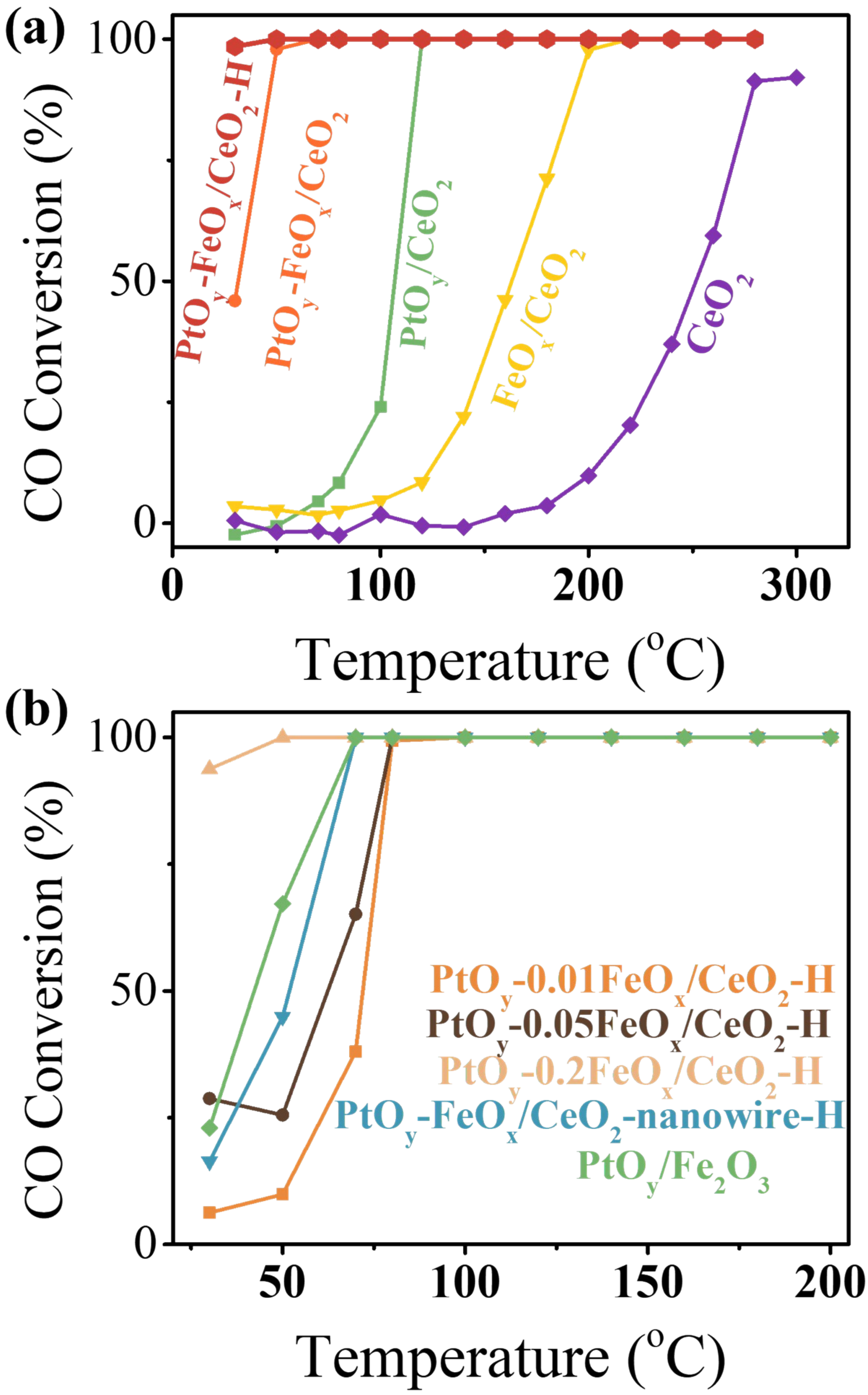

Figure S9. Catalytic performances of the samples for the model CO oxidation in 1% CO and 20% O_2 with 79% He as balance gas.

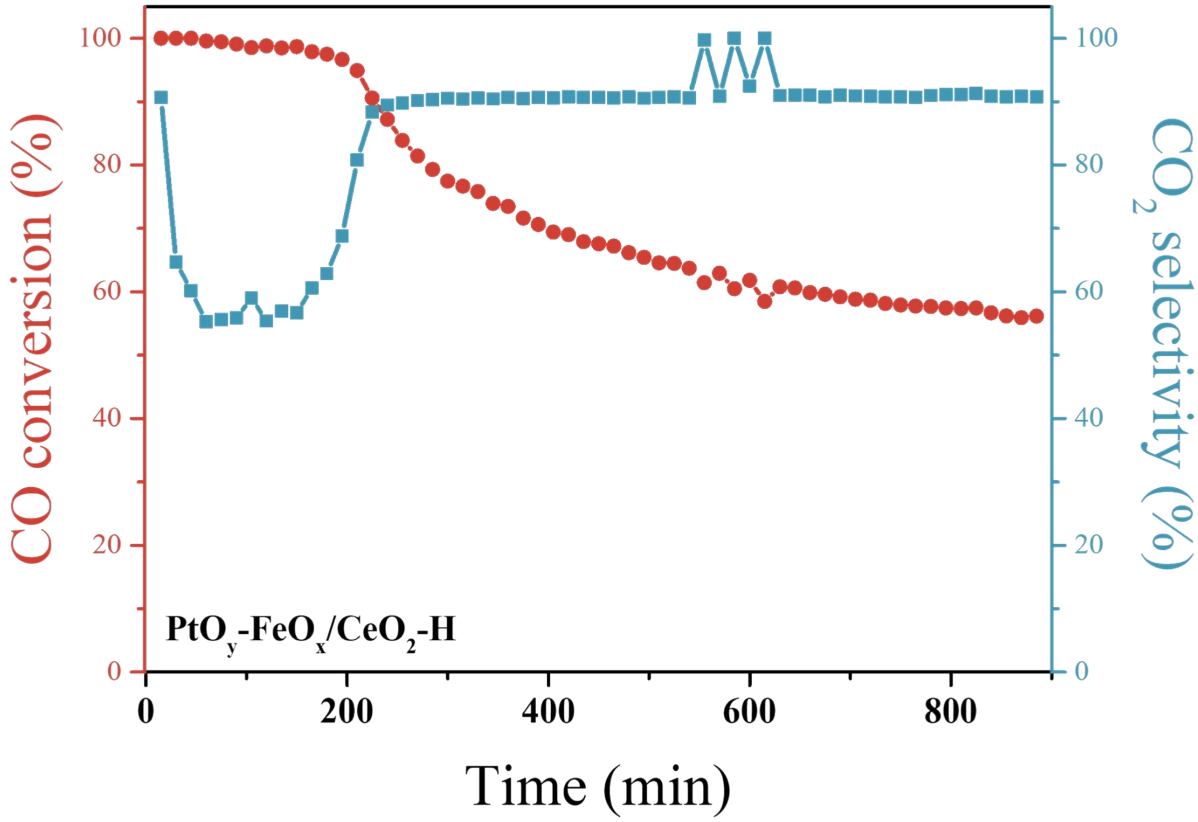

Figure S10. CO-PROX performance of PtO$_y$-FeO$_x$/CeO$_2$-H in a long time testing.

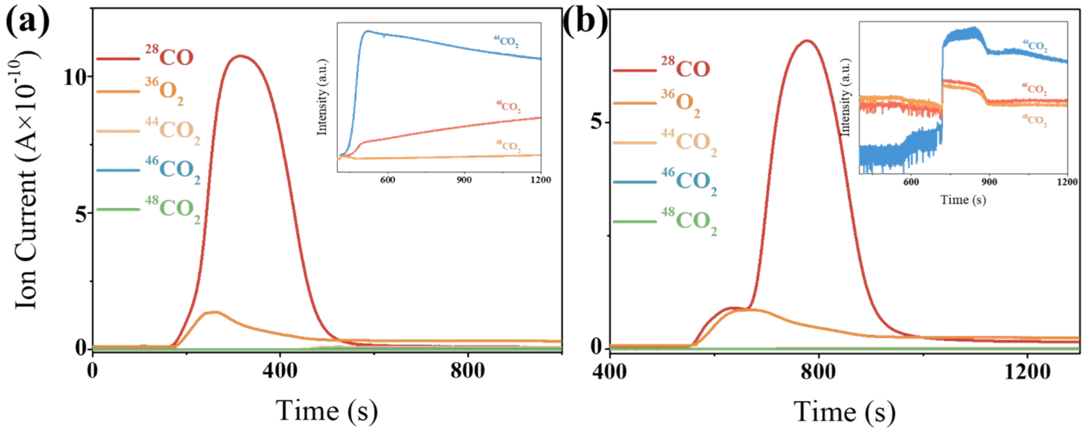

Figure S11. MS signals measured after injecting $^{36}O_2$ and ^{28}CO into reaction with the samples: PtO_y-FeO_x/CeO_2-H (left) and PtO_y-FeO_x/CeO_2 (right) measured at room temperature.

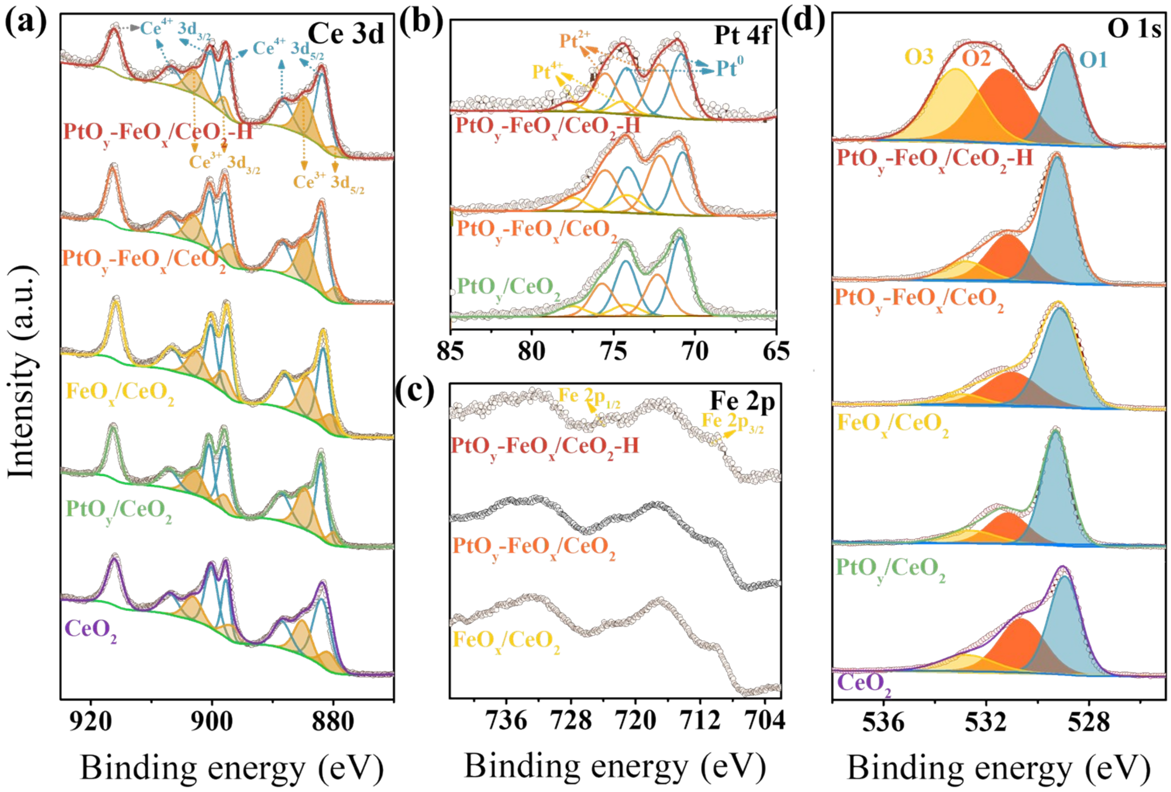

Figure S12. Core level XPS spectra of samples: (a) Ce 3d, (b) Pt 4f, (c) Fe 2p, and (d) O 1s.

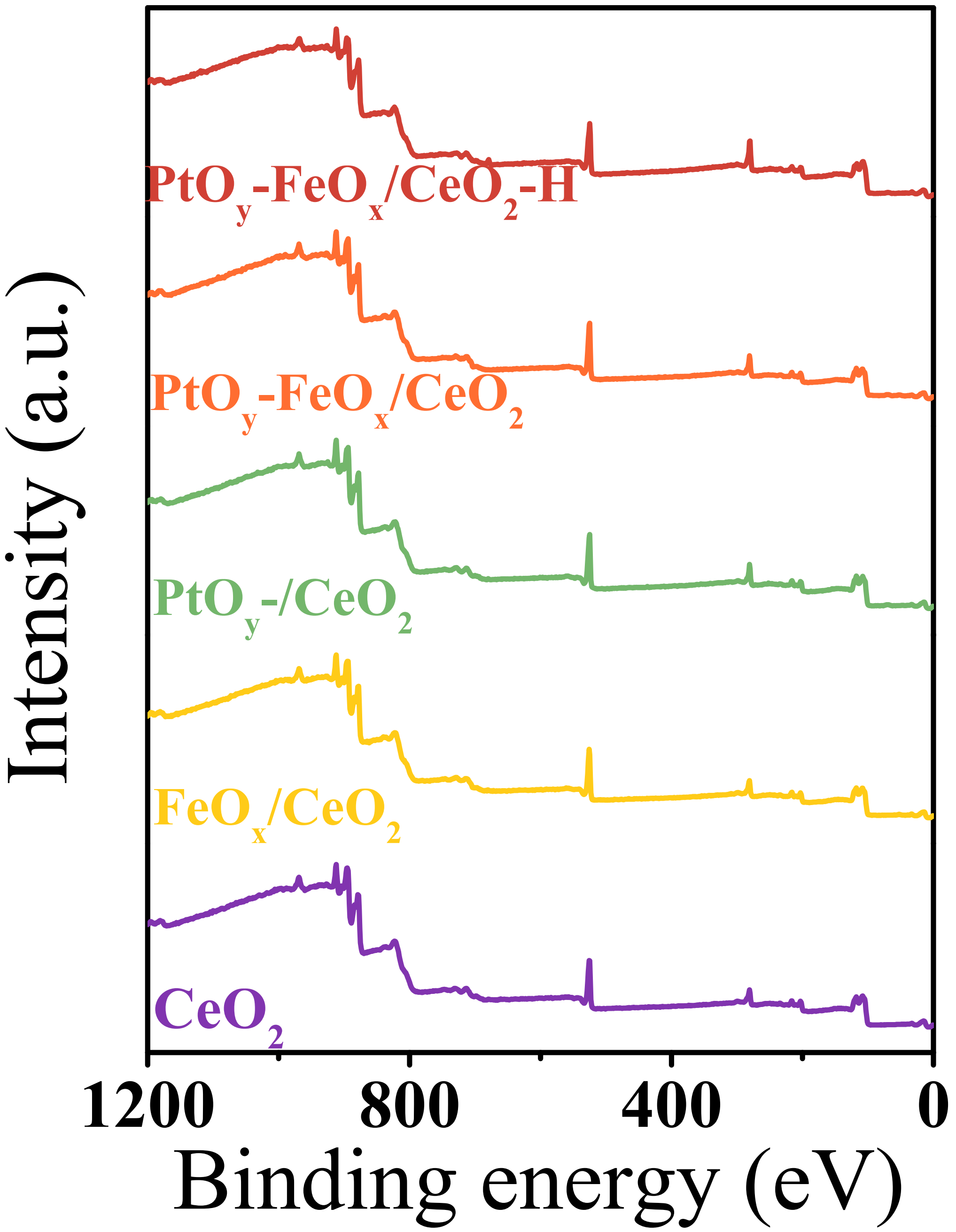

Figure S13. Survey spectra of samples.

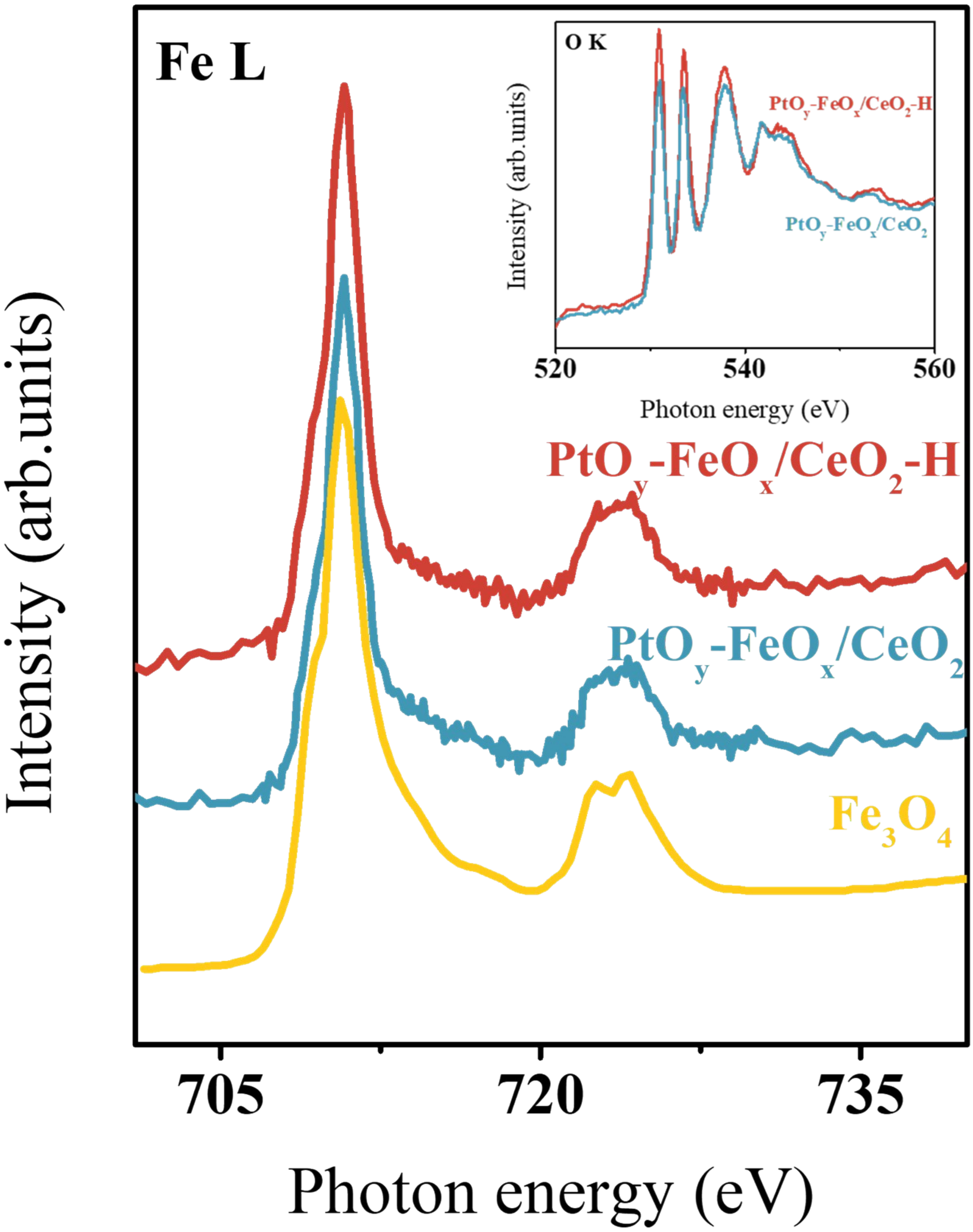

Figure S14. XANES of the samples.

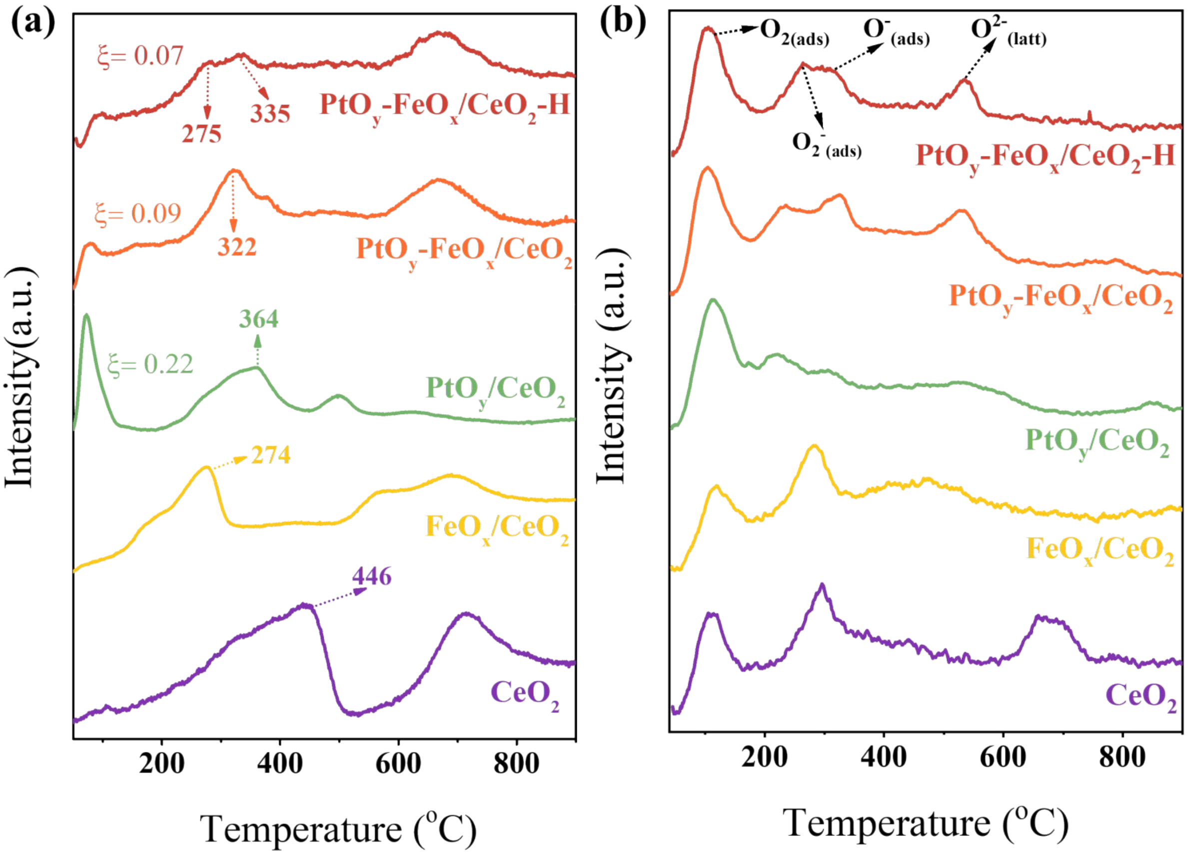

Figure S15. (a) H_2-TPR and (b) O_2-TPD profiles of the given samples. ξ in (a) represents the ratio of H_2 spillover peak to total hydrogen consumption.

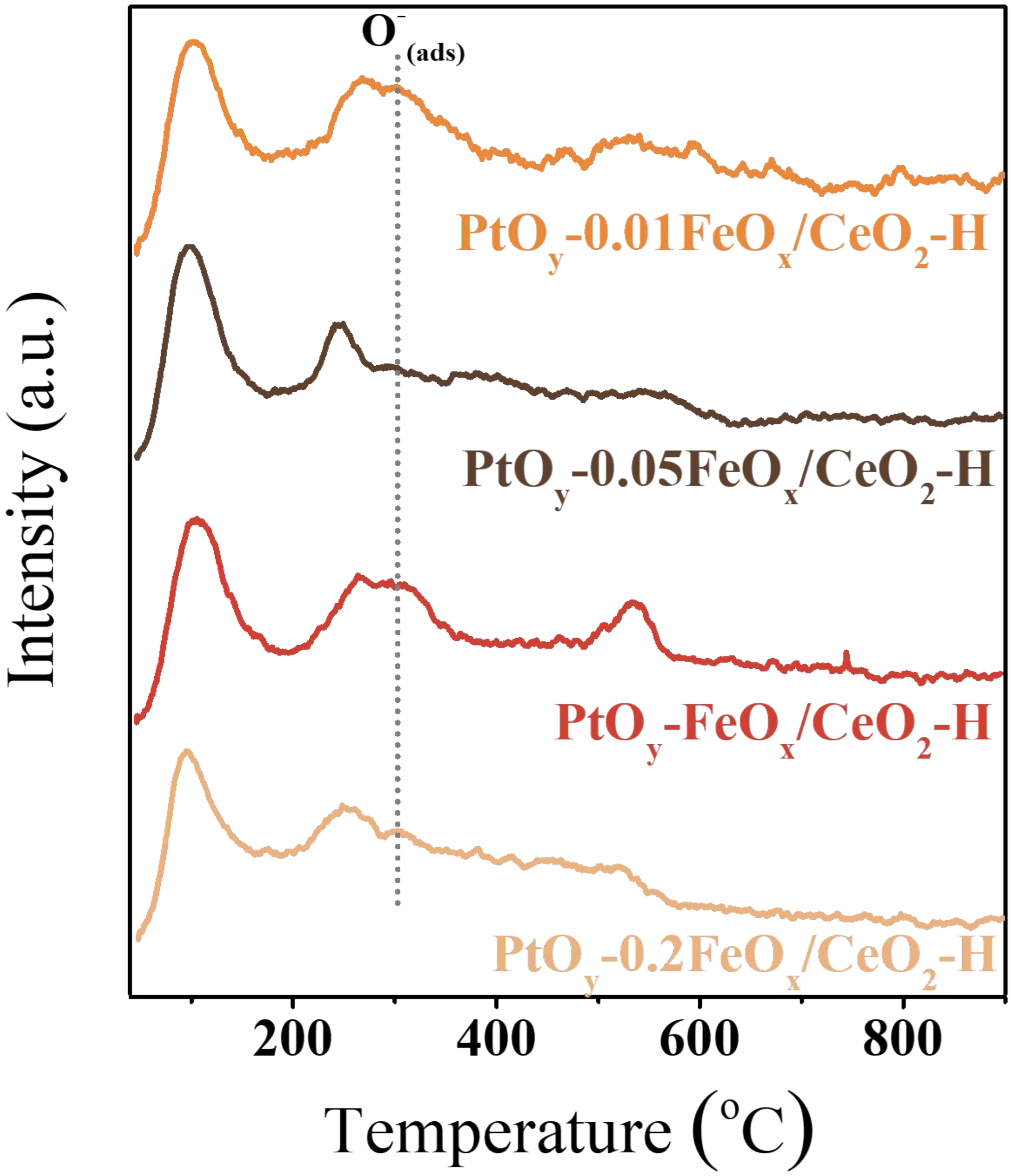

Figure S16. Comparison of O_2-TPD profiles of the samples: PtO_y-FeO_x/CeO_2-H and PtO_y-mFeO_x/CeO_2-H (m=0.01, 0.05 and 0.2).

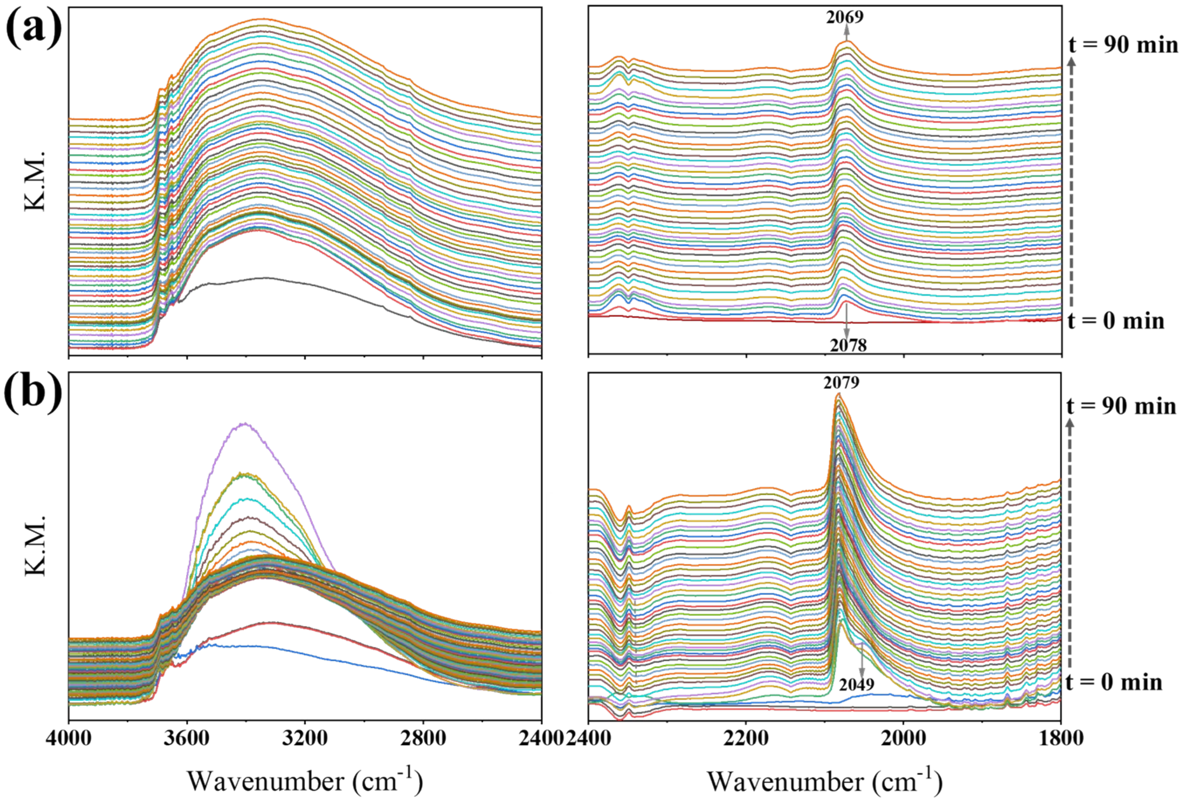

Figure S17. In situ DRIFTS spectra obtained under CO-PROX conditions (1% CO, 1.25% O2 and 50% H_2 in He balance) over the samples: (a) PtO_y-FeO_x/CeO_2-H and (b) PtO_y-FeO_x/CeO_2. The spectra were recorded at a time range of 0-90 min with an interval of 2 min.

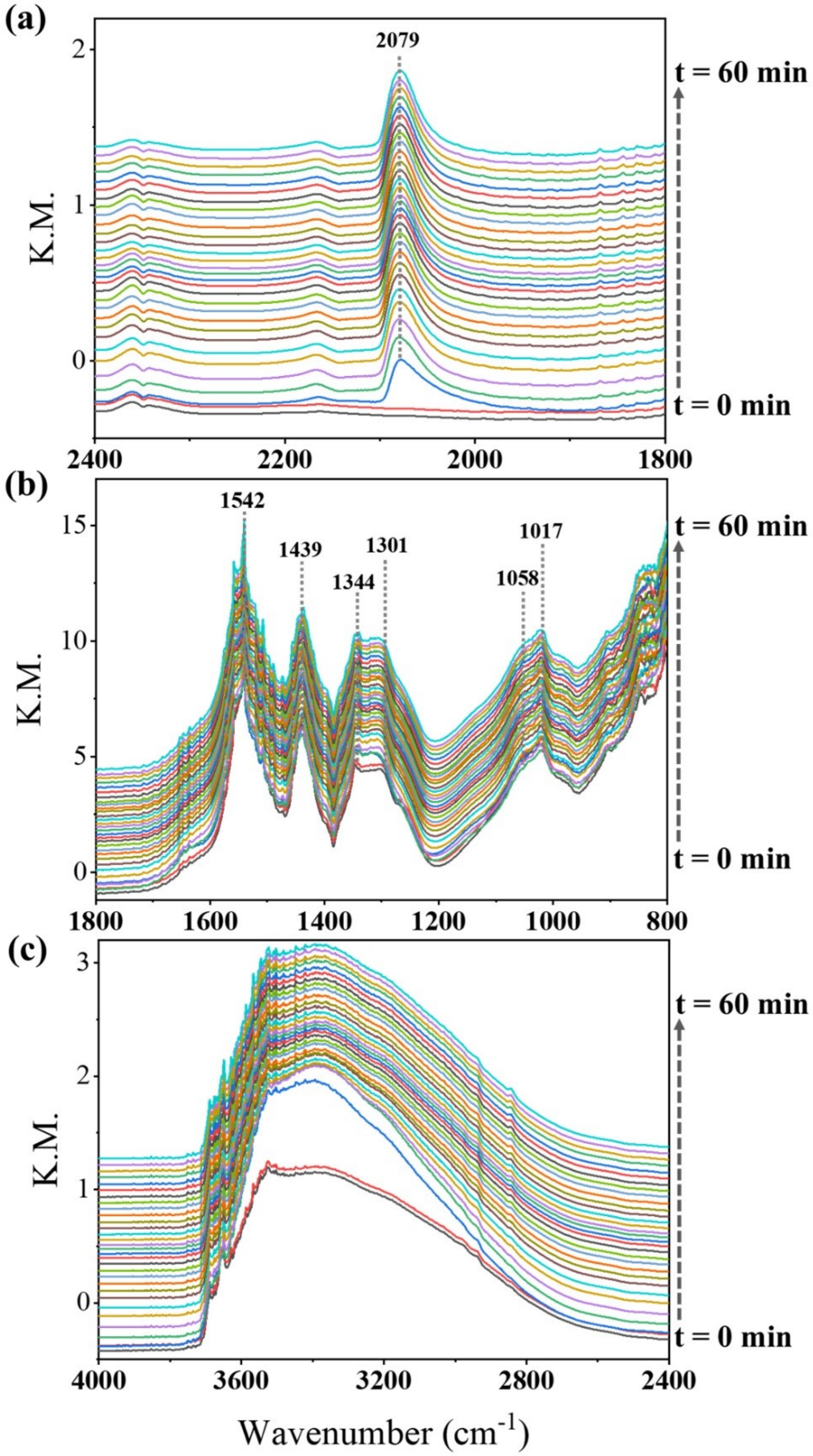

Figure S18 Temporal evolutions of DRIFTS spectra after reactive gas adsorption on PtO_y/CeO_2.

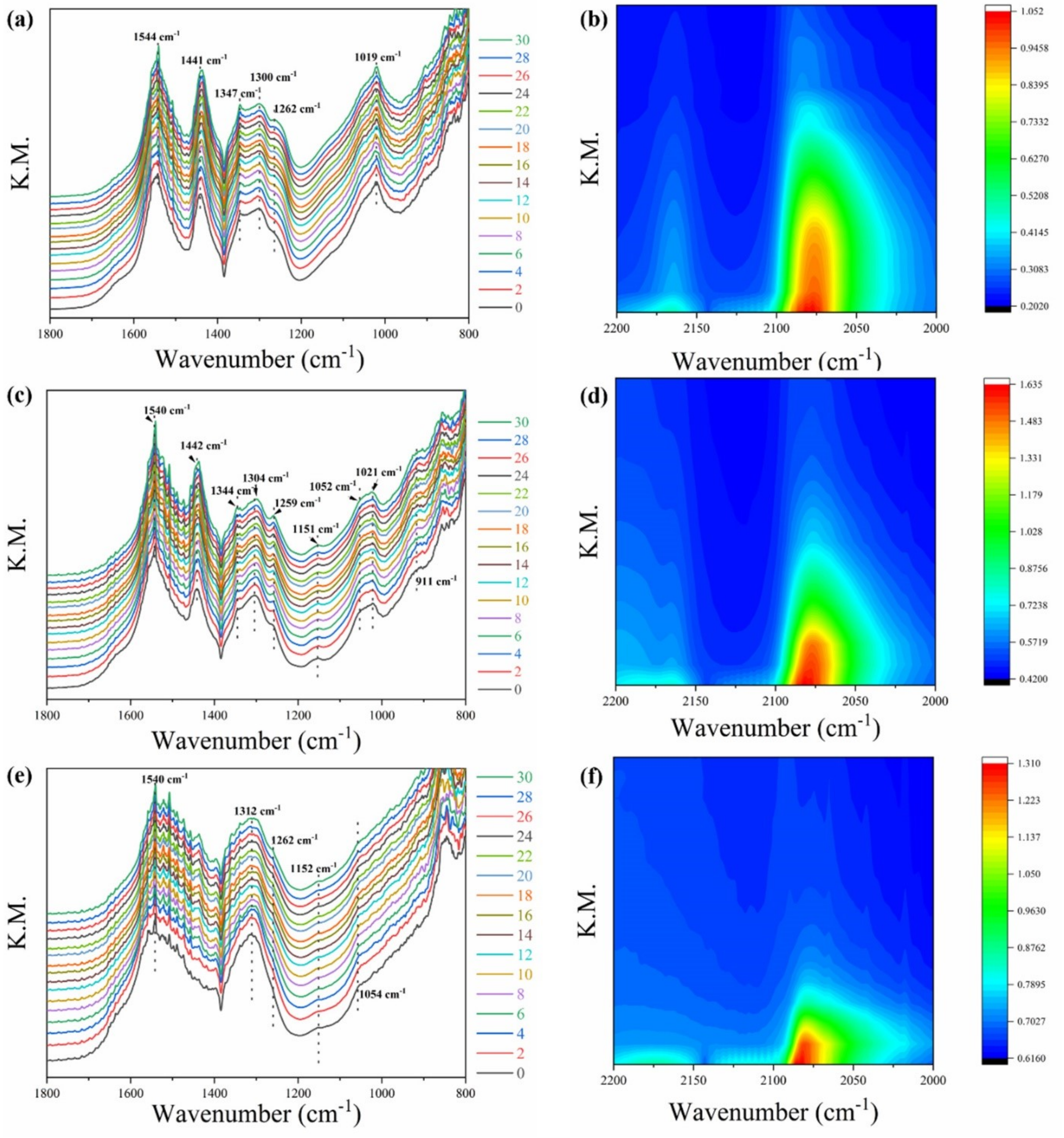

Figure S19. Temporal evolutions of DRIFTS spectra after CO saturation adsorption on samples: (a) PtO_y/CeO_2, (c) PtO_y-FeO_x/CeO_2, (e) PtO_y-FeO_x/CeO_2-H in a continuous flow of N_2. Temporal evolutions of DRIFTS isotherms after CO saturation adsorption on samples: (b) PtO_y/CeO_2, (d) PtO_y-FeO_x/CeO_2, (f) PtO_y-FeO_x/CeO_2-H in a continuous flow of N_2. The measured interval is 2 min and time range is 0-30 min.

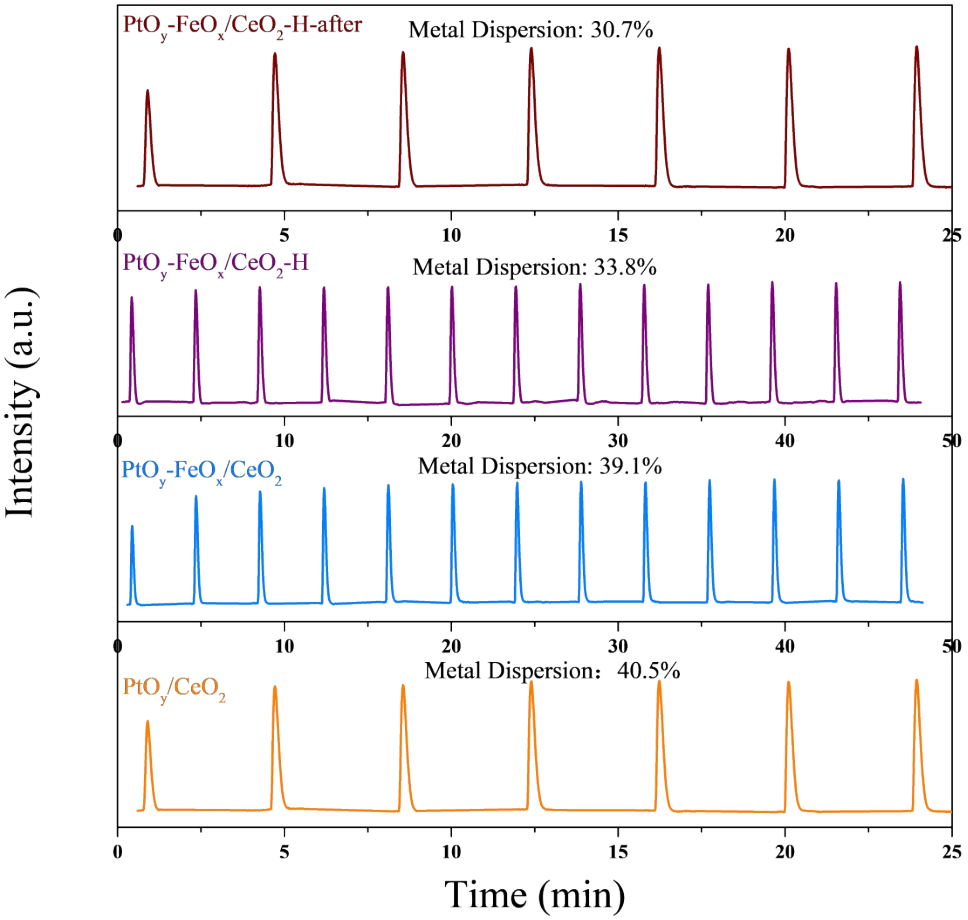

Figure S20. CO pulse adsorption profiles of the given samples.

Table S1. Lattice parameter, surface areas, grain size and stress of samples.

samples	a=b=c (Å)	BET (m^2/g)	Grain size (nm)[a]	Stress (%)[a]
CeO_2	5.414(2)	168.6	8.7	0.60
PtO_y/CeO_2	5.415(9)	161.3	8.1	0.48
FeO_x/CeO_2	5.410(9)	159.8	8.9	0.60
PtO_y-FeO_x/CeO_2	5.408(3)	149.5	9.6	0.64
PtO_y-FeO_x/CeO_2-H	5.414(1)	128.4	8.9	0.57

[a]: The grain size and lattice stress were calculated by Williams-Hall theorem using Scherrer formula with lattice stress correction. 4 strong diffractions of (111), (200), (220), and (311) were chosen to calculate.

Table S2. Comparison of performance of catalysts reported in reference and PtO_y-FeO_x/CeO_2-H.

samples	Mass of catalyst (mg)	GHSV ($mL·g_{cat}^{-1}·h^{-1}$)	Gas	T_{100}	Ref.
PtO_y-FeO_x/CeO_2-H	50	60000	1%CO,1%O_2,50%H_2 He balance	RT	This work
CuCe-Fe	300	16000	1%CO,1%O_2,50%H_2 He balance	100°C	4
1/10$Fe_{(N)}$-CuCZ	300	24000	1%CO,1%O_2,50%H_2 He balance	120°C	5
Pt/NiFeAl-600	50	60000	1%CO,20%O_2 He balance	100°C	6
Pt/CeO-S	30	200000	0.4%CO，10%O_2 Ar balance	150°C	7
Pt/Fe_3O_4	50	240000	1500ppmCO,10%O_2 N_2 balance	150°C	8
CuO/CeO_2-polyhedra	100	24000	1%CO,1.25%O_2,50%H_2 He balance	90°C	9

References

(1) R. Jain, A. S. Poyraz, D. P. Gamliel, J. Valla, S. L. Suib and R. Maric, *Appl. Catal., A*, 2015, **507**, 1-13.

(2) W. Lin, A. Herzing, C. Kiely and I. Wachs, *J. Phys. Chem. C*, 2008, **112**, 5942-5951.

(3) D. L. De Faria, S. Venâncio Silva and M. De Oliveira, *J. Raman Spectrosc.*, 1997, **28**, 873-878.

(4) J. Lu, J. Wang, Q. Zou, D. He, L. Zhang, Z. Xu, S. He and Y. Luo, *ACS Catal.*, 2019, **9**, 2177-2195.

(5) J. Wang, C. Han, X. Gao, J. Lu, G. Wan, D. He, R. Chen, K. Chen, S. He and Y. Luo, *J. Power Sources*, 2017, **343**, 437-445.

(6) J. Ding, L. Li, Y. Wang, H. Li, M. Yang and G. Li, *Nanoscale*, 2020, **12**, 14882-14894.

(7) L. Nie, D. Mei, H. Xiong, B. Peng, Z. Ren, P. Hernandez Xavier Isidro, A. DeLaRiva, M. Wang, H. Engelhard Mark, L. Kovarik, K. Datye Abhaya and Y. Wang, *Science*, 2017, **358**, 1419-1423.

(8) L. Ma, X. Chen, J. Li, H. Chang and J. W. Schwank, *Catal. Today*, 2020, **355**, 539-546.

(9) X. Guo and R. Zhou, *Catal. Sci. Technol.*, 2016, **6**, 3862-3871.